Sensitivity of Shielding Effectiveness to Nuclear Fragmentation Cross-section Errors

J.H. Heinbockel[1], S.R. Blattnig[2], F.F. Badavi[4], F.A. Cucinotta[3], G.D. Qualls[2], J.W. Wilson[2], M.S. Clowdsley[2], J. Tweed[1]

[1] Old Dominion University, Norfolk, Virginia
[2] NASA Langley Research Center, Hampton, Virginia
[3] NASA Johnson Space Center, Houston, Texas
[4] Christopher Newport University, Newport News, Virginia

Abstract

It has long been recognized that galactic cosmic rays are of such high energy that they tend to pass through available shielding materials resulting in exposure of astronauts and equipment within space vehicles and habitats. Any protection provided by shielding materials results not so much from stopping such particles but by changing their physical character by interaction with shielding material nuclei to hopefully a less dangerous species. Clearly, the fidelity of nuclear cross sections is essential to correct specification of shield design and sensitivity to cross section error is important in guiding experimental validation of cross section models and database.

We examine the Boltzmann transport equation which is used to calculate a radiation dose equivalent, with units (cSv/year), associated with various depths of shielding materials. The equivalent radiation dose is a weighted sum of contributions from protons, alpha particles, light ions, medium ions, heavy ions and neutrons. We consider production terms arising from all possible projectile-fragment interactions. The accuracy of the resulting dose equivalent is dependent upon the projectile-fragment production cross-sections. We investigate the sensitivity of the dose equivalent calculations due to an error in a production cross-section. We do this error analysis for all possible projectile-fragment combinations (14,365) to estimate the sensitivity of the shielding calculations to errors in the nuclear fragmentation cross-sections. Numerical differentiation with respect to the cross sections will be evaluated in a broad class of materials including polyethylene, aluminum and copper. We will identify the most important cross sections for further experimental study and evaluate their impact on propagated errors in shielding estimates.

Key words: HZETRN, sensitivity, shielding, fragmentation, cross-section errors

Introduction

Particle transport equations are derived from continuum mechanics principles, (Wilson et al 1991). The particle flux in a shielding material is determined by balancing the change in particle flux across a small volume element of material with gains and losses caused by nuclear collisions

within the material. The resulting equation is the well known Boltzmann equation

$$[\quad \frac{1}{A_j}\frac{}{E}S_j(E) + \quad _j(E)]\ _j(x, \quad ,E) = \quad _k \ _E dE'd\ ' \quad _{jk}(E,E', \quad , \quad ')\ _k(x, \quad ',E') \qquad (1)$$

where $_j(x, \quad ,E)$ represents the flux of type j-particles with atomic mass A_j at position x with motion in the direction having energy E. Occurring in the equation (1) are the terms $_j(E)$ which represents the macroscopic cross section in units of cm^{-1}, $S_j(E)$ representing the linear energy transfer or change in energy per unit distance. The fragmentation of the projectile and target nuclei is represented by the fragmentation cross sections $_{jk}(E,E', \quad , \quad ')$ which represents the production cross section for type j particles with energy and direction having a collision with a type k particle of energy with direction '. That is, $_{jk}$ is a cross-section, in units of cm^{-1}, for producing ion j from a collision by ion k. These cross sections are composed of three parts and can be written

$$_{jk}(E,E', \quad ., \quad ') = \ _k(E')\ _{jk}(E')\ f_{jk}(E,E', \quad , \quad ') \qquad (2)$$

where $_{jk}(E')$ represents the average number of type j particles produced by a collision with a type k particle of energy . The term $f_{jk}(E,E', \quad , \quad ')$ is the probability density distribution for producing particles of type j of energy into the direction from the collision of the type k particle with energy moving in the direction '.

The propagation of galactic cosmic rays into shielding material is described by the above Boltzmann equation. The galactic cosmic ray (GCR) transport radiation code HZETRN, (Shin et al 1992), was developed by NASA Langley Research Center around the 1980-1990 period. One of the things that this code can do is to solve a one-dimensional form of the equation (1) and use quality factors to calculate total radiation dose equivalent, in units of cSv/yr at various depths in a shielding material. The results are particularly important in determining radiation exposure of astronauts and electrical equipment on space missions. It has long been recognized that galactic cosmic rays are of such high energy that they tend to pass through available shielding materials resulting in exposure of astronauts and equipment within space vehicles and habitats. Any protection provided by shielding materials results not so much from stopping such particles but by changing their physical character by interaction with shielding material nuclei to hopefully less dangerous species. An understanding of these processes can be discerned by conducting various shielding simulations using the HZETRN computer code. Clearly, the fidelity of the nuclear cross sections are essential to correct specification of shield design and sensitivity to cross section error is important in guiding experimental validation of cross section models and the construction of cross section databases.

In this paper we examine a one-dimensional form of the Boltzmann transport equation (1), which is solved by way of the HZETRN code subject to the galactic cosmic rays and the 1977 solar minimum environment. The HZETRN code calculates a radiation dose equivalent, with units of (cSv/yr), associated with various depths within a shielding material. The radiation dose equivalent is a weighted sum of contributions from protons, alpha particles, light ions , medium ions, heavy ions and neutrons. We consider production terms arising from 170 possible projectile-fragment cross-sections. The isotopes considered in the interactions are listed in the table 1. The accuracy of the resulting dose equivalent is dependent upon the projectile-fragment production

cross-sections. We investigate the sensitivity of the dose equivalent calculations due to production cross section errors using sensitivity analysis. We do this error analysis for all possible projectile-fragment combinations (14,365) to estimate the sensitivity of the shielding calculations to errors in the nuclear fragmentation cross-sections. Numerical differentiation with respect to the cross sections is evaluated for the selected shield materials of polyethylene, aluminum and copper. We will identify the most important cross sections for further experimental study. The purpose of the investigation is to evaluate the cross sections impact on propagated errors in shielding estimates associated with radiation protection studies.

Error Analysis

Let H denote the equivalent total dose calculated by the HZETRN code. If an error $_{ij} > 0$ is introduced into the fragmentation cross sections $_{ij}$ used to calculate of the equivalent total dose, then what kind of errors can be expected in the predicted radiation dose equivalent? By employing a Taylor series expansion one can show that

$$H(\ _{ij} + \ _{ij}) - H(\ _{ij}) = \sum_i \sum_j \frac{H}{\ _{ij}}\ _{ij} + \text{higher order terms.} \qquad (3)$$

We neglect the higher order terms of the Taylor series expansion and consider a single error associated with an i,j combination where i and j have fixed values. If the first order term is large, then the higher order terms would need to be examined. By introducing an error into a single cross section we can obtain a numerical approximation for just one term from the right-hand side of equation (3). By going through all i, j combinations one obtains a numerical approximation for each term on the right-hand side of the Taylor series. We can then use these numerical approximations for the derivatives to formulate a Monte Carlo simulation given by

$$H(\ _{ij} + \ _{ij}\ _{ij}) = H(\ _{ij}) + \sum_i \sum_j \frac{H}{\ _{ij}}\ _{ij}\ _{ij} \qquad (4)$$

where $_{ij}$ are random variates from a normal distribution In this way one can model the effect of errors in calculating the total dose equivalent.

The figure 1 illustrates the resulting errors in the equivalent dose at various depths within an aluminum shield due to the introduction of a single error in a specific k-projectile, j-fragment cross section. For each given j,k value the cross section $_{jk}$ was replaced by 2 $_{jk}$. This was done for all 14,365 combinations of j and k. Also illustrated in these figures is the summation of fragment errors associated with a given projectile k. The figures 2 and 3 are similar figures for copper and polyethylene respectively.

Results and Discussion

The highest five peaks occurring in the figures 1,2 and 3, ordered from highest to lowest, correspond to the isotopes of $_{26}Fe^{56}$, $_{8}O^{16}$, $_{14}Si^{28}$, $_{12}Mg^{24}$ and $_{6}C^{12}$. These elements are the five most abundant heavier elements in the Galactic cosmic ray composition. The equivalent dose errors for aluminum, copper and polyethylene are more pronounced along the line of lower J-values and along the line where $j \quad k$. This is due to projectile interaction with shield material which causes few nucleon removal followed by resultant particle movement into the material

showing up as the errors near the $j = k$ line. Consequently, the equivalent dose errors correspond to few nucleon removal followed by projectile fragment continuation after interaction. Studies which incorporate errors from all sources indicate low overall errors produced in the dose equivalent calculations. This is also indicative of the results obtain from figure 4, where all cross sections were set equal to zero.

Similar sensitivity studies for an aluminum shield can be found by Townsend et al 1992, where in that study the production cross-sections $_{jk}$ where replaced by p $_{jk}$, where p varied from 0.5 to 1.5 and the equivalent dose calculations where compared with the nominal values obtained when p=1.

One might conclude that the results of this study suggest that for the 1977 solar minimum environment and GCR environment, the dose equivalent is not very sensitive to errors in the production cross sections. However, one can not conclude that secondary particle production is not important in general. Note that the production cross section errors can greatly affect the shielding requirements for a given dose limit. This is illustrated by the horizontal lines depicted in the figure 4. Particle production from lighter nucleon removal has the largest effect on dose equivalent from the HZETRN code. The largest change in dose equivalent is due to light, medium and heavy ion drop off with depth into shielding material. Emphasis on the most abundant elements in the Galactic cosmic rays and their particle interaction with the shield material is the most important issue in determining dose equivalent predictions.

Future efforts are being directed toward developing additional physics and mathematics for describing the propagation of particles through a shielding medium.

Acknowledgement: Research was sponsored by NASA grant NAG-1-03075.

References

[1] Wilson, J.W. Wilson, L.W. Townsend, W. Schimmerling, G.S. Khandalwal, F. Khan, J.E. Nealy, F.A. Cucinotta, L.C. Simonsen, J.L. Shinn, J.W. Norbury, Transport Methods and Interactions for Space Radiations, NASA Reference Publication-1257, (1991).

[2] Shinn, J.L. Shinn, J.W. Wilson, An Efficient HZETRN (A Galactic Cosmic Ray Transport Code), NASA Technical Paper-3147, April, 1992.

[3] Townsend, L.W. Townsend, F.A. Cucinotta, J.L. Shinn, J.W. Wilson, Effects of Fragmentation Parameter Variations on Estimates of Galactic Cosmic Ray Exposure-Dose Sensitivity Studies for Aluminum Shields , NASA Technical Memorandum-4386, July 1992.

[4] Cucinotta, F.A., Sagouti, P.B., Hu, X., et al, Physics of the Isotope Dependence of Galactic Cosmic Ray Fluence Behind Shielding. NASA TP-2003—210792, 2003.

HZETRN Indices for Isotope Atomic Weight and Charge			
I	A	Z	Isotope
1	1	0	n
2	1	1	$_{1}H^{1}$
3	2	1	$_{1}H^{2}$
4	3	1	$_{1}H^{3}$
5	3	2	$_{2}He^{3}$
6	4	2	$_{2}He^{4}$
7	6	2	$_{2}He^{6}$
8	6	3	$_{3}Li^{6}$
9	7	3	$_{3}Li^{7}$
10	7	4	$_{4}Be^{7}$
11	8	3	$_{3}Li^{8}$
12	8	5	$_{5}B^{8}$
13	9	3	$_{3}Li^{9}$
14	9	4	$_{4}Be^{9}$
15	9	5	$_{5}B^{9}$
16	10	4	$_{4}Be^{10}$
17	10	5	$_{5}B^{10}$
18	10	6	$_{6}C^{10}$
19	11	4	$_{4}Be^{11}$
20	11	5	$_{5}B^{11}$
21	11	6	$_{6}C^{11}$
22	12	5	$_{5}B^{12}$
23	12	6	$_{6}C^{12}$
24	12	7	$_{7}N^{12}$
25	13	5	$_{5}B^{13}$
26	13	6	$_{6}C^{13}$
27	13	7	$_{7}N^{13}$
28	14	6	$_{6}C^{14}$
29	14	7	$_{7}N^{14}$
30	14	8	$_{8}O^{14}$
31	15	6	$_{6}C^{15}$
32	15	7	$_{7}N^{15}$
33	15	8	$_{8}O^{15}$
34	16	7	$_{7}N^{16}$
35	16	8	$_{8}O^{16}$
36	17	7	$_{7}N^{17}$
37	17	8	$_{8}O^{17}$
38	17	9	$_{9}F^{17}$
39	18	8	$_{8}O^{18}$
40	18	9	$_{9}O^{18}$
41	18	10	$_{10}Ne^{18}$
42	19	8	$_{8}O^{19}$
43	19	9	$_{9}F^{19}$
44	19	10	$_{10}Ne^{19}$
45	20	8	$_{8}O^{20}$
46	20	9	$_{9}F^{20}$
47	20	10	$_{10}Ne^{20}$
48	21	9	$_{9}F^{21}$
49	21	10	$_{10}Ne^{21}$
50	21	11	$_{11}Na^{21}$
51	22	10	$_{10}Ne^{22}$
52	22	11	$_{11}Na^{22}$
53	23	10	$_{10}Ne^{23}$
54	23	11	$_{11}Na^{23}$
55	23	12	$_{12}Mg^{23}$
56	24	10	$_{10}Ne^{24}$
57	24	11	$_{11}Na^{24}$

HZETRN Indices for Isotope Atomic Weight and Charge			
I	A	Z	Isotope
58	24	12	$_{12}Mg^{24}$
59	25	11	$_{11}Na^{25}$
60	25	12	$_{12}Mg^{25}$
61	25	13	$_{13}Al^{25}$
62	26	11	$_{11}Na^{26}$
63	26	12	$_{12}Mg^{26}$
64	26	13	$_{13}Al^{26}$
65	26	14	$_{14}Si^{26}$
66	27	12	$_{12}Mg^{27}$
67	27	13	$_{13}Al^{27}$
68	27	14	$_{14}Si^{27}$
69	28	12	$_{12}Mg^{28}$
70	28	13	$_{13}Al^{28}$
71	28	14	$_{14}Si^{28}$
72	29	13	$_{13}Al^{29}$
73	29	14	$_{14}Si^{29}$
74	29	15	$_{15}P^{29}$
75	30	13	$_{13}Al^{30}$
76	30	14	$_{14}Si^{30}$
77	30	15	$_{15}P^{30}$
78	30	16	$_{16}S^{30}$
79	31	14	$_{14}Si^{31}$
80	31	15	$_{15}P^{31}$
81	31	16	$_{16}S^{31}$
82	32	14	$_{14}Si^{32}$
83	32	15	$_{15}P^{32}$
84	32	16	$_{16}S^{32}$
85	33	14	$_{14}Si^{33}$
86	33	15	$_{15}P^{33}$
87	33	16	$_{16}S^{33}$
88	33	17	$_{17}Cl^{33}$
89	34	15	$_{15}P^{34}$
90	34	16	$_{16}S^{34}$
91	34	17	$_{17}Cl^{34}$
92	35	15	$_{15}P^{35}$
93	35	16	$_{16}S^{35}$
94	35	17	$_{17}Cl^{35}$
95	35	18	$_{18}Ar^{35}$
96	36	16	$_{16}S^{36}$
97	36	17	$_{17}Cl^{36}$
98	36	18	$_{18}Ar^{36}$
99	37	16	$_{16}S^{37}$
100	37	17	$_{17}Cl^{37}$
101	37	18	$_{18}Ar^{37}$
102	37	19	$_{19}K^{37}$
103	38	16	$_{16}S^{38}$
104	38	17	$_{17}Cl^{38}$
105	38	18	$_{18}Ar^{38}$
106	38	19	$_{19}K^{38}$
107	38	20	$_{20}Ca^{38}$
108	39	17	$_{17}Cl^{39}$
109	39	18	$_{18}Ar^{39}$
110	39	19	$_{19}K^{39}$
111	39	20	$_{20}Ca^{39}$
112	40	18	$_{18}Ar^{40}$
113	40	19	$_{19}K^{40}$
114	40	20	$_{20}Ca^{40}$

HZETRN Indices for Isotope Atomic Weight and Charge			
I	A	Z	Isotope
115	41	18	$_{18}Ar^{41}$
116	41	19	$_{19}K^{41}$
117	41	20	$_{20}Ca^{41}$
118	42	18	$_{18}Ar^{42}$
119	42	19	$_{19}K^{42}$
120	42	20	$_{20}Ca^{42}$
121	42	21	$_{21}Sc^{42}$
122	43	19	$_{19}K^{43}$
123	43	20	$_{20}Ca^{43}$
124	43	21	$_{21}Sc^{43}$
125	44	20	$_{20}Ca^{44}$
126	44	21	$_{21}Sc^{44}$
127	44	22	$_{22}Ti^{44}$
128	45	20	$_{20}Ca^{45}$
129	45	21	$_{21}Sc^{45}$
130	45	22	$_{22}Ti^{45}$
131	46	20	$_{20}Ca^{46}$
132	46	21	$_{21}Sc^{46}$
133	46	22	$_{22}Ti^{46}$
134	46	23	$_{23}V^{46}$
135	47	21	$_{21}Sc^{47}$
136	47	22	$_{22}Ti^{47}$
137	47	23	$_{23}V^{47}$
138	48	21	$_{21}Sc^{48}$
139	48	22	$_{22}Ti^{48}$
140	48	23	$_{23}V^{48}$
141	48	24	$_{24}Cr^{48}$
142	49	22	$_{22}Ti^{49}$
143	49	23	$_{23}V^{49}$
144	49	24	$_{24}Cr^{49}$
145	50	22	$_{22}Ti^{50}$
146	50	23	$_{23}V^{50}$
147	50	24	$_{24}Cr^{50}$
148	50	25	$_{25}Mn^{50}$
149	51	23	$_{23}V^{51}$
150	51	24	$_{24}Cr^{51}$
151	51	25	$_{25}Mn^{51}$
152	52	23	$_{23}V^{52}$
153	52	24	$_{24}Cr^{52}$
154	52	25	$_{25}Mn^{52}$
155	53	24	$_{24}Cr^{53}$
156	53	25	$_{25}Mn^{53}$
157	53	26	$_{26}Fe^{53}$
158	54	24	$_{24}Cr^{54}$
159	54	25	$_{25}Mn^{54}$
160	54	26	$_{26}Fe^{54}$
161	55	25	$_{25}Mn^{55}$
162	55	26	$_{26}Fe^{55}$
163	55	27	$_{27}Co^{55}$
164	56	26	$_{26}Fe^{56}$
165	56	27	$_{27}Co^{56}$
166	56	28	$_{28}Ni^{56}$
167	57	26	$_{26}Fe^{57}$
168	57	27	$_{27}CO^{57}$
169	57	28	$_{28}Ni^{57}$
170	58	28	$_{28}Ni^{58}$

Table 1. Projectile-fragmentation isotopes

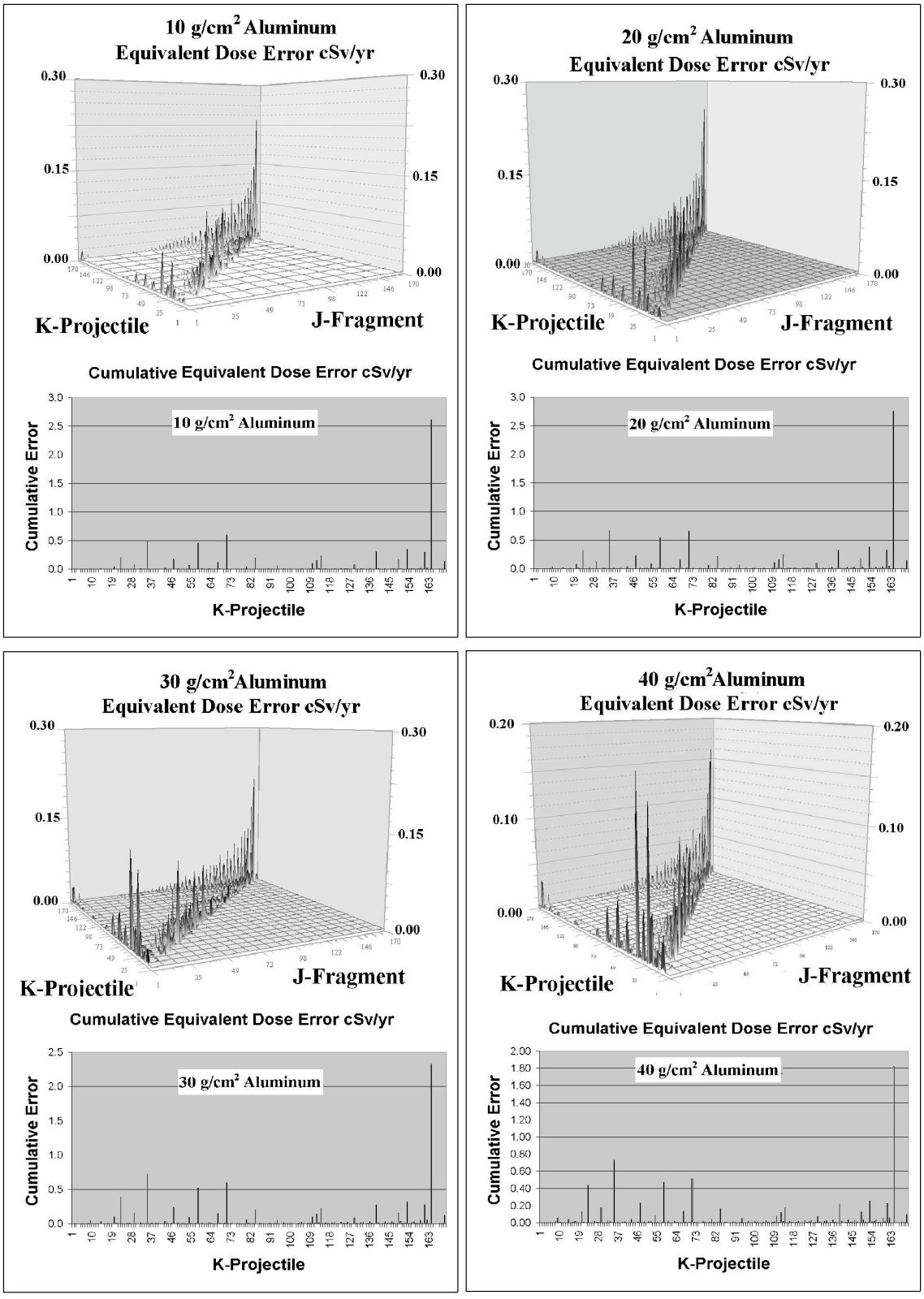

Figure 1. Error and cumulative error graphs for Aluminum shield at various depths

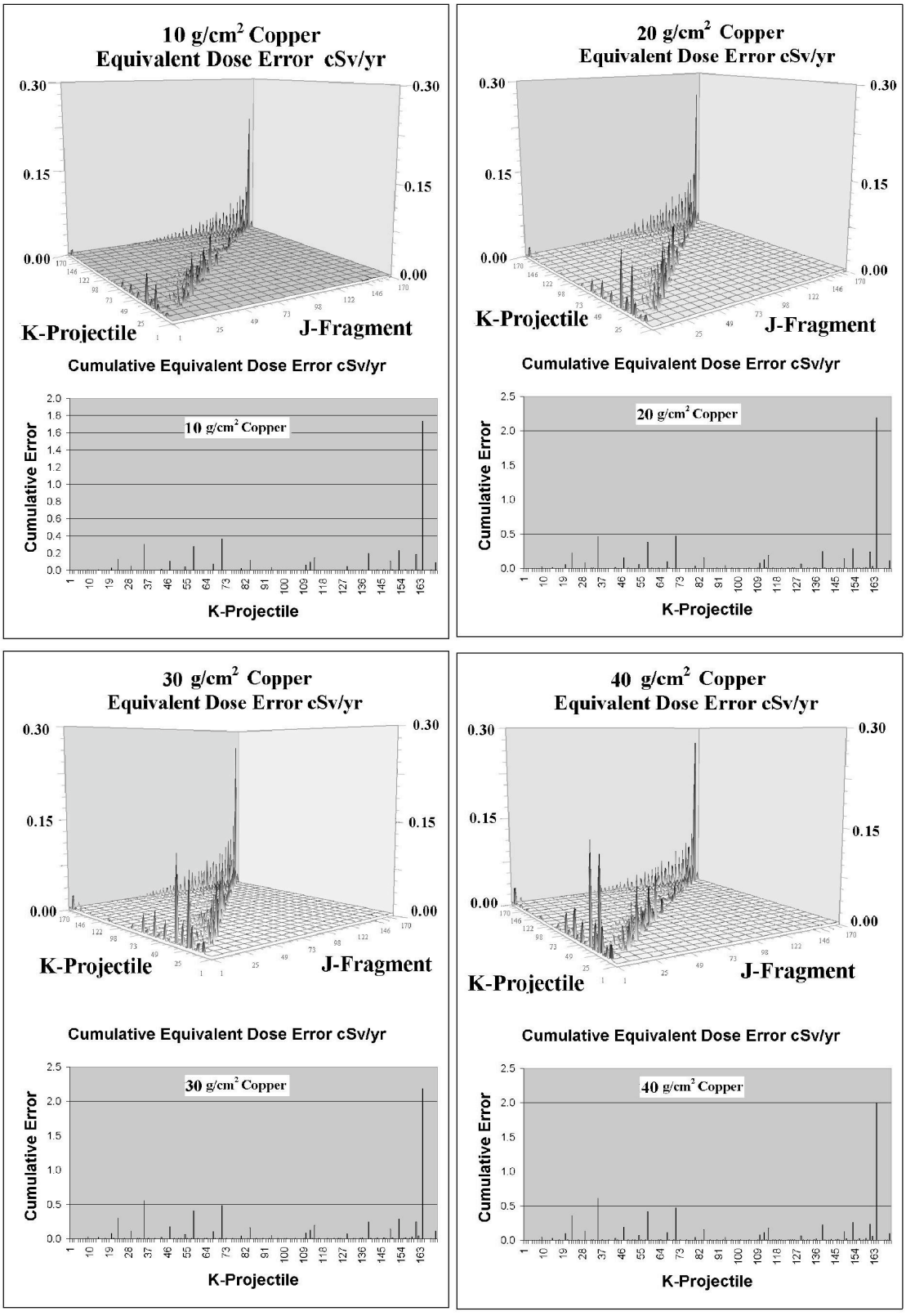

Figure 2. Error and cumulative error graphs for Copper shield at various depths

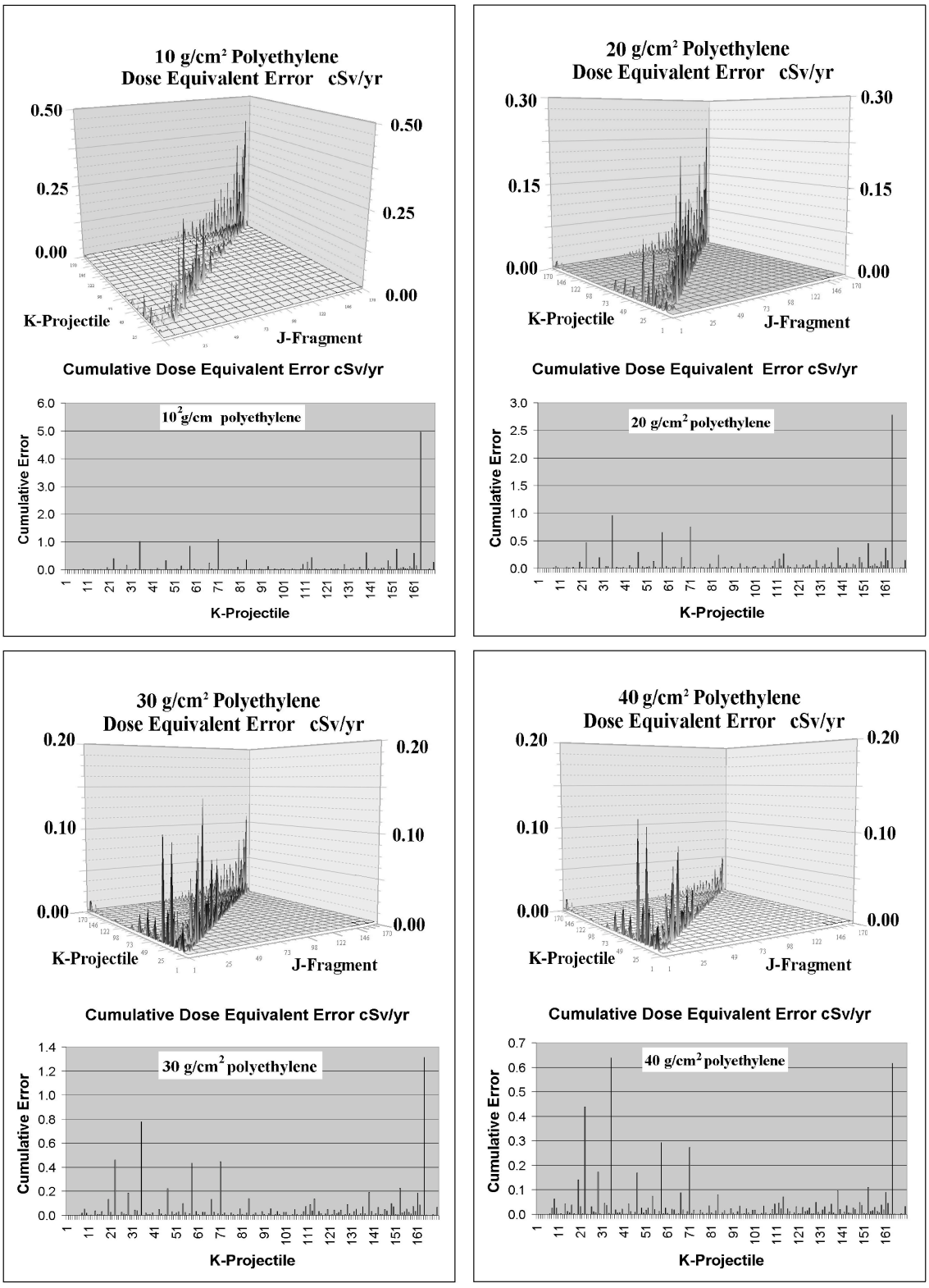

Figure 3. Error and cumulative error graphs for polyethylene shield at various depths

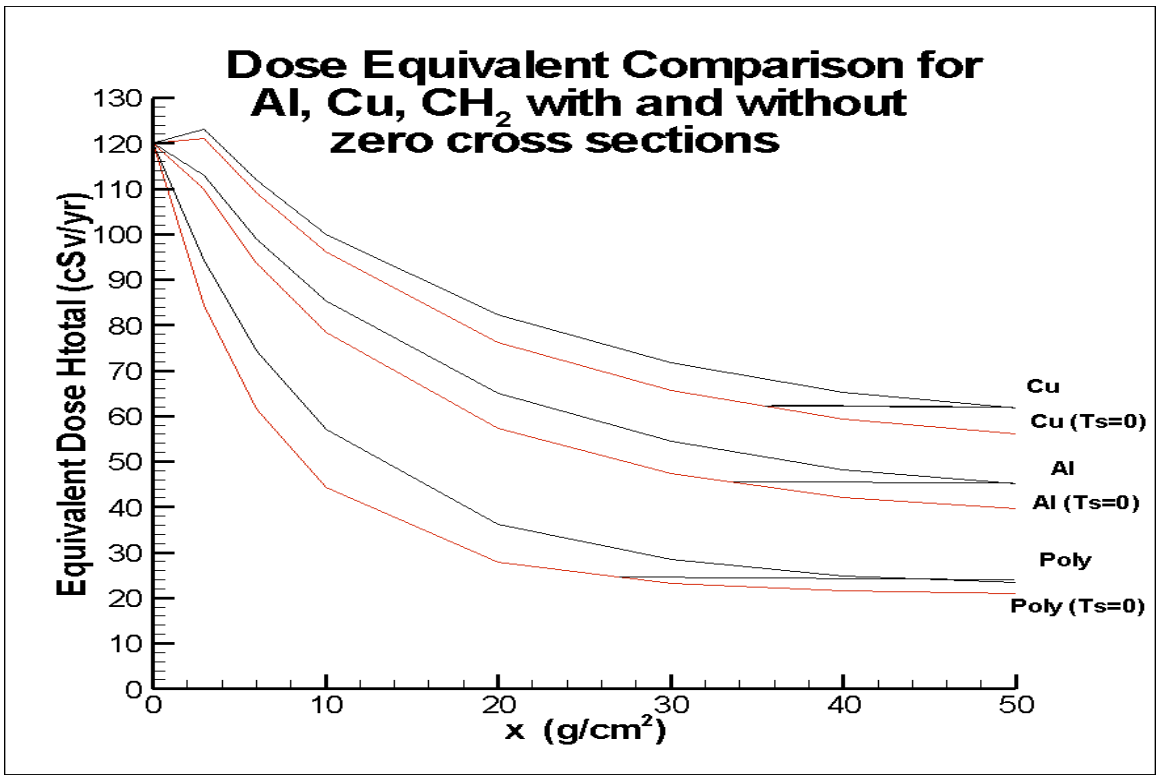

Figure 4. Dose equivalent comparison with and without production cross-sections equal to zero.

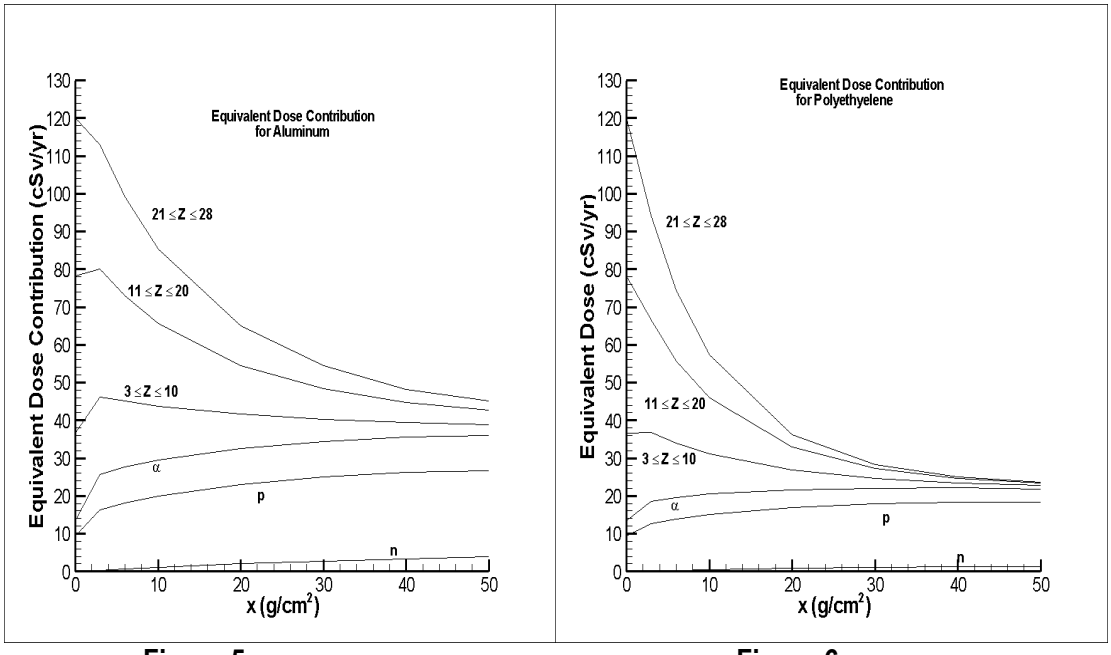

Figure 5.
Dose contribution Aluminum

Figure 6.
Dose contribution polyethyelene